

## K-shell photoabsorption spectra of N<sub>2</sub> and N<sub>2</sub>O using synchrotron radiation

A. Bianconi\* and H. Petersen†

*Stanford Synchrotron Radiation Laboratory, Department of Applied Physics, Stanford University, Stanford, California 94305*

Frederick C. Brown

*Department of Physics, University of Illinois at Urbana-Champaign, Urbana, Illinois 61801*

R. Z. Bachrach

*Xerox Palo Alto Research Center, Palo Alto, California 94304*

(Received 31 January 1978)

The total photoionization cross section of the 1s level of nitrogen in N<sub>2</sub> and N<sub>2</sub>O molecules has been measured using monochromatized synchrotron radiation. High-resolution spectra in the range  $390 < \hbar\omega < 450$  eV were recorded. A broadband in the continuum at 9.4 eV above the ionization threshold, due to the *f*-type shape resonance, has been measured with high resolution. The data are compared with theoretical calculations of photoionization cross section. Recent Hartree-Fock calculations in the static-exchange approximation agree better than earlier results, which employed the multiple-scattering method.

### I. INTRODUCTION

Total photoabsorption and photoionization cross-section measurements for carbon, nitrogen, and oxygen near the *K* threshold are of interest, but lie in a difficult spectral region. We have recently measured photoabsorption above the *K* edge in a series of small molecules containing carbon and nitrogen using monochromatized synchrotron radiation. We have presented the data on methane and fluoromethane elsewhere,<sup>1</sup> and in this work we discuss measurements above the nitrogen *K* edge.

Detailed theoretical calculations of the *K*-shell photoionization cross section of N in N<sub>2</sub> have been given recently by Dehmer and Dill,<sup>2</sup> who used a multiple-scattering method (MSM or *X<sub>2</sub>*), and by Rescigno and Langhoff,<sup>3</sup> who used Stieltjes-Tchebycheff calculations in the static-exchange approximation. The photoabsorption cross section can be calculated with these methods in the region near the edge where the usual theory of extended x-ray absorption fine structures (EXAFS)<sup>4</sup> does not apply. For comparison with theory, we have measured the absolute photoabsorption cross section of N<sub>2</sub> and N<sub>2</sub>O over a large energy range with high resolution using synchrotron radiation. Heretofore, measurements of the N<sub>2</sub> and N<sub>2</sub>O nitrogen *K* absorption were performed using synchrotron radiation with photographic registration<sup>5</sup> and also by electron energy loss (ELS) using 2.5-keV electrons.<sup>6-8</sup> In both cases quantitative comparison with theory is difficult: for photographic registration, because of the nonlinear response of photographic plates, and in the case of ELS, because of the excitation process and finite range of observed scattering angles. Nitrogen *K*-absorption

data has also been obtained using x-ray bremsstrahlung from a tungsten anode.<sup>9,10</sup> However, the resolution was not very high and the results were limited to the near-edge region. The present work confirms the very high intensity of the first peak and determines the strength and shape of the broad maximum in the continuum. Extended x-ray absorption fine structure oscillations far above the edge are not observed in the limited observation range available above threshold in this experiment. The differences between N<sub>2</sub>O and N<sub>2</sub> are discussed.

### II. EXPERIMENTAL METHOD

Photon-absorption data were obtained by transmission measurements as a function of gas pressure using monochromatized synchrotron radiation emitted by the storage ring SPEAR. For this purpose the 2-m grazing incidence monochromator ("grasshopper")<sup>11</sup> on the 4° line at the Stanford Synchrotron Radiation Laboratory was utilized. The fixed exit beam from this instrument was focused by a bent toroidal mirror at 2° grazing so as to pass through the gas-absorption apparatus<sup>12</sup> with thin transparent windows. The 3-mm-diam windows consisted of 1000-Å-thick titanium films supported by 80%-transparent nickel mesh. These windows enclosed a 13.5-cm-long static cell. They separated the gas region (pressure up to 5 Torr) from the surrounding ultrahigh-vacuum chamber (10<sup>-9</sup>–10<sup>-8</sup> Torr), which was connected through the monochromator to SPEAR vacuum. Numerous sensors and automatic valves protected the line in case of a leak. A high degree of isolation was achieved through the use of differential pumping and because the monochromator employs ~10-μm entrance and

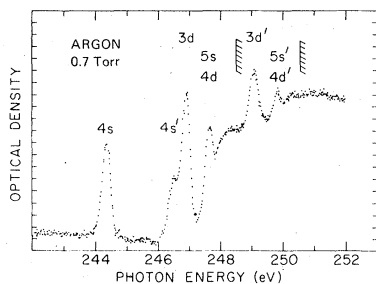


FIG. 1.  $L_{2,3}$  absorption edge of argon gas recorded in first order with about 0.7 Torr pressure in the gas cell. Bandwidth of spectrometer  $\sim 0.3$  eV at 250 eV.

exit slits.

A double "chevron" channel plate detector was located beyond the gas cell within the high-vacuum chamber. This detector could be operated either in a photon counting mode or as an indicator of average current. Transmission data were recorded, and the results were reduced with an on-line computer.<sup>13</sup> For example, the data were corrected for stray light by making scans of both gas sample and reference (empty cell) out to beyond 1-keV photon energy, where there was little true flux due to cutoff of reflecting surfaces. These scans were then displayed as intensity versus photon energy. The background was extrapolated into the region of interest and subtracted from both sample and reference data, after which the optical density and absorption cross section were computed. Absolute gas pressures were measured with a high-precision Wallace and Tiernan gauge, but due to compounding of errors, measured cross sections in Mb are uncertain to perhaps  $\pm 20\%$ .

For the present relatively high energy work, a 2400-lines/mm Bausch and Lomb replica grating

(catalogue No. 35-52-37-800) was used. A resolution of about 0.4 eV was achieved in the energy range of interest. This is demonstrated by a scan in first order of the  $L_{2,3}$  absorption edge of argon gas at 244 eV. Figure 1 shows the raw data taken in less than 10 min. The first line in this spectrum is the spin-orbit split  $2p_{3/2} \rightarrow 4s$  Rydberg transition of the rare gas. The features shown in Fig. 1 were resolved by Nakamura *et al.*<sup>5</sup> using a grazing incidence spectrometer in third order. The energy they report for the  $2p_{3/2} \rightarrow 4s$  line of  $244 \pm .04$  eV was used for adjustment and calibration of our monochromator. After setting up the instrument, these lines were reproducible within the point density of Fig. 1, which was about 50 points/eV.

### III. RESULTS AND DISCUSSION

Figure 2 shows the original data points of the  $N_2$   $K$ -absorption spectrum between 400 and 425 eV. The absolute cross section in Mb is plotted as a function of photon energy in eV. Note that the first peak has an oscillator strength much stronger than the rest of the spectrum, which has been multiplied by a factor of 10. The first line is more than 30 times as intense as the remaining structure and continuum. The energy positions of peaks are reported in Table I. A discussion of the spectrum can be divided into two sections: (i) the discrete part below the ionization potential [determined by electron spectroscopy for chemical analysis (ESCA) as 409.9 eV (Ref. 14)]; and (ii) the continuum above the ionization potential. Clearly the spectrum does not show a simple  $1s \rightarrow np$  Rydberg series converging to a continuum, as should be the case for atomic nitrogen. After the  $K$  edge the oscillator strength does not de-

TABLE I. Energy of observed features in the  $K$ -absorption spectrum of nitrogen gas along with assignment of excited states.

Gas	Feature	Photon energy (eV)	Energy relative to the $K$ -edge ionization potential (eV)	Excited-state symmetry	Calculated energy (eV) <sup>a</sup>
$N_2$	A	401.3 <sup>b</sup>	-8.6	$\pi_g$	-7.20
	B	406.1	-3.8	$\sigma_g$	-3.50
	C	407.3	-2.6	$\pi_u$	-2.58
	D	408.9	-1.0	$\pi_g; \pi_u$	-1.30
	E	410.0	+0.1		
	F	415.0	+5.1		
	G	419.3	+9.4	$\sigma_u$	10.90

<sup>a</sup> Theory of Dehmer and Dill (Ref. 2).

<sup>b</sup> The energy scale is established by extrapolation from a one-point calibration at the argon  $L$  edge (Ref. 11). Nakamura *et al.*, (Ref. 5) give this energy as 400.8 eV. The two numbers agree within the accuracy of the respective calibrations.

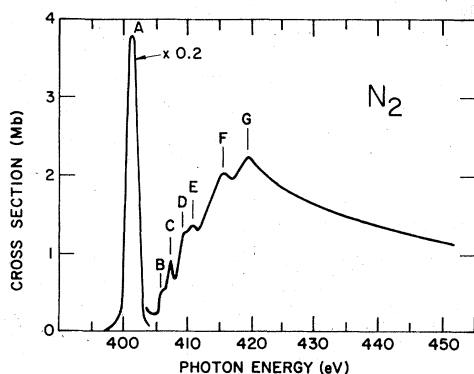


FIG. 2. N<sub>2</sub> *K*-photoabsorption spectrum. Since peak A is much stronger than all other features, the theoretical and experimental spectra below 403 eV have been reduced by 0.2, i.e., the maximum of experimental peak A is about 17.4 mB.

crease but rises to a broad peak G.

Figure 3 shows the N<sub>2</sub> *K*-absorption spectrum up to 450-eV photon energy along with twice the photoionization cross section of atomic nitrogen, indicated by  $2 \times \sigma(N)$ . The theoretical predictions are given from two different approaches, according to Refs. 2 and 3. Also shown by the vertical lines under NO levels are the positions of expected peaks on the basis of the well-known  $Z+1$  analogy.<sup>15</sup> This is based on the assumption that the effect of the hole created by the photoabsorp-

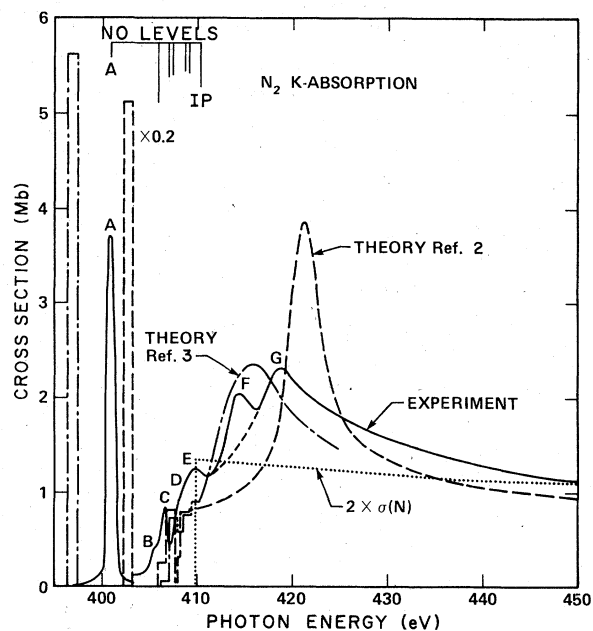


FIG. 3. *K*-edge of N<sub>2</sub> is shown in comparison to the theory of Dehmer and Dill (Ref. 2) and Rescigno and Langhoff (Ref. 3).

tion process in the 1s shell can be simulated by adding one positive charge to the core. The N<sub>2</sub> *K* spectrum has, therefore, to be compared to the valence-band spectrum of NO.<sup>16</sup> Although the energetic positions of structure in both spectra are in reasonable agreement (the first NO level as positioned at peak A), the shape of the N<sub>2</sub> *K* spectrum differs dramatically from the intensity distribution usually observed in valence-band spectra.

The theoretical curve included as a dashed line in Fig. 3 represents results from the calculation of the N<sub>2</sub> *K*-absorption cross section using the MSM,<sup>2</sup> while the dash-dot curve is from Ref. 3. Note that peak A is more than 10 times as intense as peak B in both experiment and theory! According to Ref. 2, the high oscillator strength of this first peak is caused by a centrifugal-barrier effect which manifests itself as a shape resonance in the high-*l* components of the final-state wave functions. The peak A corresponds to the first member of the  $\pi_g$  final-state Rydberg series.<sup>7,17</sup> Its dominant *d*-symmetric term (partial-wave expansion) is coupled by the molecular field to the *p* wave, which is initially produced by photoabsorption of a *K* electron in an essentially atomic field. Because of its predominantly *d* nature, the  $\pi_g$  final state is concentrated within the centrifugal barrier for *d*-symmetric wave functions. This leads to a high overlap of initial and final states and thus to the observed strong oscillator strength, which is in good agreement with the MSM calculation.

The peak A as well as higher-lying structure all lie above the valence-band ionization channels. In the case of the lower-energy valence-band absorption, the first peak is observed as a continuum shape resonance 2.4 eV above the ionization limit.<sup>18,19</sup> The high-energy A peak of Fig. 3 occurs at -8.6 eV below the *K* edge. The structures B, C, and D correspond to Rydberg excited states and can be reasonably correlated with features in the theoretical curve. The assignment of the final-state symmetries according to Ref. 2 are reported in Table I. Above the *K* edge the band F at 415 eV has been attributed to double excitation.<sup>8</sup>

Comparing the continuum shape resonance G at 419.3 eV and the absorption to beyond 450 eV to theory,<sup>2,3</sup> qualitative agreement is found with the theoretical prediction of the shape resonance in the continuum.<sup>2,3</sup> On the other hand, the energy position of the observed resonance occurs at a slightly lower energy than the calculated peak of Ref. 2 (9.4 eV compared to 10.9 eV above the ionization potential). It should be noted that the distance between the observed peaks A and G is the same as that calculated, namely, 18 eV.

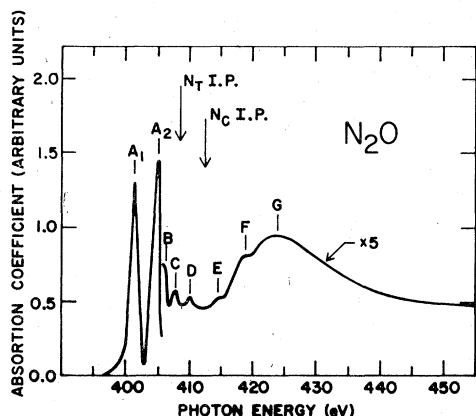


FIG. 4.  $N_2O$   $K$ -photoabsorption spectrum. The lines show the ionization potential of the "terminal" nitrogen,  $N_T$ , and that of the central nitrogen  $N_C$ . The spectrum above 405 eV has been increased by a factor of 5.

Using the multiple-scattering theory, Dehmer and Dill<sup>2</sup> have found that the  $l=3$  component of the final-state wave function has a resonance near  $G$  mainly due to the  $\sigma_u$  channel of the excited electron. An  $f$ -like final-state wave function oriented along the molecular axis penetrates the molecular centrifugal barrier, and a substantial overlap with the  $1s$  core orbital occurs. These higher- $l$  components arise from scattering as in EXAFS theory, which involves the backscattering of outgoing  $p$  waves from neighboring atoms. Scattering of the outgoing wave is also involved in the near-edge structure, but for energies  $\leq 50$  eV above the ionization potential, the actual excited state in the anisotropic molecular field must be calculated. We were not able to observe any EXAFS oscillation above the peak  $G$  in the limited energy range. Dehmer and Dill<sup>2</sup> suggest that they should be weak and unobservable in the case of  $N_2$ . The only molecular EXAFS effect in this energy range is a  $N_2$  cross section slightly lower than the  $2 \times N$  cross section; both curves join smoothly at about 190 eV above the ionization potential.<sup>2</sup>

In comparing the theoretical results of Refs. 2 and 3 with experiment, one sees that the approach of Rescigno and Langhoff<sup>3</sup> appears to be in better agreement with experiment than the  $X\alpha$  calculation,<sup>2</sup> both for energetic peak position and cross-section magnitude.

Figure 4 shows the  $K$ -photoabsorption spectrum of the nitrous oxide molecule ( $N_2O$ ). (See also Table II.) Unlike the diatomic ( $N_2$ ) molecular spectrum, two strong peaks,  $A_1$  and  $A_2$ , are found below the  $K$ -ionization potential. In fact, the  $N_2O$  molecule can be written as  $N_T N_C O$ , where  $N_C$  and  $N_T$  are two inequivalent nitrogens with different core binding energies and ionization potentials.<sup>15</sup> For  $N_C$  the

TABLE II. Energy of observed features in the  $K$ -absorption spectrum of  $N_2O$ .

Gas	Feature	Photon energy (eV)
$N_2O$	$A_1$	401.16
	$A_2$	404.92
	$B$	406.90
	$C$	408.00
	$D$	410.00
	$E$	414.60
	$G$	423.50

$K$ -edge ionization potential is 412.5 and for  $N_T$ , 408.5.<sup>14</sup> The peaks  $A_1$  and  $A_2$  can be attributed to transitions to the same  $d$ -wave component of the  $p$ -type ionization channel, as peak  $A$  in the nitrogen molecule (from the  $1s$  levels of  $N_T$  and  $N_C$ , respectively). The peaks  $B$ ,  $C$ , and  $D$  are due to the two superimposed Rydberg series extending up to their respective ionization thresholds. Again, by analogy with the  $N_2$  case, the peak  $G$  can be attributed to a "shape resonance" in the continuum. Also, in this case no EXAFS modulations above the  $G$  peak were observed. In the case of the  $N_2O$  molecule, direct comparison to the calculated cross-section values cannot be made due to the lack of such a calculation. However, concerning the distribution of the oscillator strength below and above the ionization threshold, the  $N_2O$   $K$ -photoabsorption spectrum is very similar to the  $N_2$  curve.

In conclusion, we have measured the photoionization cross section for inner-shell transitions in the continuum of  $N_2$  and  $N_2O$ . For  $N_2$  qualitative agreement is found with theory although the energy relative to the  $K$  edge of the first excited state  $A$  as well as that of the shape resonance  $G$  is found to be slightly different from the calculated energies.<sup>2,3</sup> The  $N_2O$  spectrum is discussed and compared with the  $N_2$  spectrum. Finally, we remark that the observed high-resolution photoabsorption spectra are in close agreement with electron-loss spectra.<sup>8</sup>

#### ACKNOWLEDGMENTS

The authors appreciate the assistance and support of the Director and staff of the Stanford Synchrotron Radiation Laboratory which is supported by the National Science Foundation in cooperation with the U. S. Energy Research and Development Administration. This project is supported by the National Science Foundation under Contract No. NSF DMR73-07692 in cooperation with the Stanford Linear Accelerator Center and

the U. S. Energy Research and Development Administration. The present work was also supported in part by the National Science Foundation under Grant No. 76-20644. We thank

Herman Winick for his encouragement and the loan by SSRL of a turbomolecular pump. Thanks are also due to H. A. Six, J. C. McMEnamin, and M. Hecht for help with the measurements.

\*Present address: Istituto di Fisica, Università di Camerino, Camerino, Italy.

†On leave from: DESY, Hamburg, W. Germany.

<sup>1</sup>F. C. Brown, R. Z. Bachrach, and A. Bianconi, *Chem. Phys. Lett.* **54**, 425 (1978).

<sup>2</sup>D. Dill and J. L. Dehmer, *Phys. Rev. Lett.* **35**, 313 (1975); J. L. Dehmer and D. Dill, *J. Chem. Phys.* **65**, 6327 (1976).

<sup>3</sup>T. N. Rescigno and P. W. Langhoff, *Chem. Phys. Lett.* **51**, 65 (1977).

<sup>4</sup>R. Kronig, *Z. Phys.* **70**, 317 (1931); C. A. Ashley and S. Doniach, *Phys. Rev. B* **11**, 1279 (1975).

<sup>5</sup>M. Nakamura, M. Sasanuma, S. Sato, M. Watanabe, H. Yamashita, Y. Iguchi, A. Ejiri, S. Nakai, S. Yamaguchi, T. Sagawa, Y. Nakai, and T. Oshio, *Phys. Rev.* **178**, 80 (1969).

<sup>6</sup>M. J. van der Wiel and Th. M. El-Sherbini, *Physica* **59**, 453 (1972).

<sup>7</sup>C. R. Wright, C. E. Brion, and M. J. van der Wiel, *J. Electron Spectrosc.* **1**, 457 (1972-1973); M. J. van der Wiel, R. B. Kay, and Ph. E. v.d. Leeuw (unpublished).

<sup>8</sup>G. R. Wight and C. E. Brion, *J. Electron. Spectrosc.*

**3**, 191 (1974).

<sup>9</sup>E. S. Gluskin, A. P. Sadovskii, and L. N. Mazala, *Zh. Sturkt. Khim.* **14**, 739 (1973).

<sup>10</sup>A. S. Vinograd, B. Shlarbaum, and T. M. Zimkina, *Opt. Spectrosc.* **36**, 658 (1974) [*Opt. Spectrosc.* **36**, 383 (1974)].

<sup>11</sup>F. C. Brown, R. Z. Bachrach, and N. Lien, *Nucl. Instrum. Methods* (to be published).

<sup>12</sup>R. Z. Bachrach, A. Bianconi, and F. C. Brown, *Nucl. Instrum. Methods* (to be published).

<sup>13</sup>R. Z. Bachrach, 1976 Quebec Summer Workshop on Synchrotron Radiation (unpublished).

<sup>14</sup>K. Siegbahn *et al.*, *ESCA Applied to Free Molecules* (North-Holland, Amsterdam, 1969).

<sup>15</sup>W. H. E. Schwartz, *Angew. Chem. Int. Ed. Eng.* **13**, 454 (1974).

<sup>16</sup>O. Edquist *et al.*, *Ark. Fys.* **40**, 439 (1970).

<sup>17</sup>M. B. Robin, *Chem. Phys. Lett.* **31**, 140 (1975).

<sup>18</sup>H. Ehhardt, L. Langhaus, F. Lindner, and H. S. Taylor, *Phys. Rev.* **173**, 222 (1968).

<sup>19</sup>M. Krauss and F. H. Mies, *Phys. Rev. A* **1**, 1592 (1970).